Breast imaging with ultrasound tomography: Update on a comparative study with MR

Bryan Ranger, Peter Littrup, Neb Duric, Cuiping Li, Steven Schmidt, Olsi Rama and Lisa Bey-Knight
Karmanos Cancer Institute, Wayne State University, 4100 John R. Street, Detroit, MI 48201

ABSTRACT

The objective of this study is to present imaging parameters and display thresholds of an ultrasound tomography (UST) prototype in order to demonstrate analogous visualization of overall breast anatomy and lesions relative to magnetic resonance (MR). Thirty-six women were imaged with MR and our UST prototype. The UST scan generated sound speed, attenuation, and reflection images and were subjected to variable thresholds then fused together into a single UST image. Qualitative and quantitative comparisons of MR and UST images were utilized to identify anatomical similarities and mass characteristics. Overall, UST demonstrated the ability to visualize and characterize breast tissues in a manner comparable to MR without the use of IV contrast. For optimal visualization, fused images utilized thresholds of 1.46±0.1 km/s for sound speed to represent architectural features of the breast including parenchyma. An arithmetic combination of images using the logical .AND. and .OR. operators, along with thresholds of 1.52±0.03 km/s for sound speed and 0.16±0.04 dB/cm for attenuation, allowed for mass detection and characterization similar to MR.

Keywords: breast, lesion, cancer, ultrasound tomography, MRI

1. INTRODUCTION

Breast magnetic resonance (MR) imaging has now become the preferred screening choice for women who are at a high risk to develop cancer, and is accepted as an important adjunctive examination to mammography and ultrasound (US) for evaluation of breast cancer (1). The efficacy of MR in investigating tumor size and extent is largely due to its high sensitivity and moderate specificity for masses over 5 mm, including invasive ductal carcinoma (IDC) and ductal carcinoma in situ (DCIS) (2). By analyzing morphology and enhancement characteristics, breast MR imaging provides qualitative and quantitative data of vascularization in order to differentiate between benign and cancerous lesions (3). In the face of these positive attributes, however, MR scanners are extremely costly to house and maintain, require specialized staff for operation, and have relatively long scan times (4).

Such disadvantages have limited the widespread use of MR for screening of the general population, as well as use in an array of diagnostic and staging choices. Accordingly, a modality that can rival MR's image quality while obviating some of the difficulties that MR presents could have a significant societal impact. Breast ultrasound tomography (UST), which can provide operator-independent and reproducible scanning, shows considerable promise as an alternative to MR (5-9). UST can accurately portray several acoustic properties of insonified tissue including margin definition, tissue elasticity, sound speed, and attenuation (10) for potential improvements in benign and malignant tissue characterization.

Building off a preliminary study (11), we have now expanded our assessment of whether UST can generate images comparable to MR. This paper presents detailed parameters that have been developed to improve image fusion methods and visualization of various architectural features of the breast as well as provide an effective means of mass characterization. Specific thresholds were determined and evaluated for UST imaging using acoustic parameters of reflection, sound speed, and attenuation in preparation for future multi-center clinical trials and a commercial product.

Medical Imaging 2011: Ultrasonic Imaging, Tomography, and Therapy, edited by Jan D'hooge, Marvin M. Doyley,
Proc. of SPIE Vol. 7968, 79680M · © 2011 SPIE · CCC code: 1605-7422/11/$18 · doi: 10.1117/12.878922

2. METHODS

2.1 Patient Recruitment and MR Dataset

Thirty-six patients were recruited at Karmanos Cancer Institute's (KCI) Alexander J. Walt Comprehensive Breast Center and given both MRI and UST breast exams. Patients were recruited based on prior US and/or mammogram findings of focal mass effect. Each patient was scanned with our clinical UST prototype after mammography and standard US exams, but before US-guided biopsy, as previously described (5-9). MRI was chosen as the gold standard for comparison due to its established accuracy and its ability to image the whole breast in manner similar to that of the acoustic prototype. MRI scans were received in axial-sliced stacks and were then re-sliced in *ImageJ* (12) into coronal views to match the native format of the UST acquisitions. The dataset included all MRI data, including T1- and T2-weighted, fat-subtracted, and contrast enhanced images. We used gadolinium-enhanced, fat-subtracted T1-weighted images to define the volume and extent of cancer in this study. T2-weighted images also helped define benign lesions such as cysts. The dataset represents a variety of breast shapes, patient ages, breast densities, and contains both benign and cancerous lesions. All imaging procedures were performed under an institutional review board-approved protocol, and in compliance with HIPAA.

2.2 UST Device and Data Acquisition

The principles and techniques of the UST device were described in detail previously (5-9). The device is markedly different than that of other imaging modalities such as mammography and conventional ultrasound. The patient is positioned face-down on the examination bed with the breast situated through a hole leading to a water tank. The breast is suspended into the water tank where it is scanned by a ring-array US transducer. Water, because it has a well-defined sound speed close to that of breast tissue, serves as the coupling medium between the breast and transducer. A 20-cm-diameter ring transducer, which operates at a frequency of 2 MHz, encircles the breast and scans from the patient's chest wall to nipple region by the means of a motorized gantry. The ring consists of 256 elements that both emit and receive the ultrasound signals. One complete scan consists of approximately 30-115 tomographic slices of the breast at 1 mm separation. The entire scanning process takes approximately 1 minute.

Three types of images are produced from the raw data using tomographic reconstruction algorithms. Sound speed images are based on the arrival times of acoustic signals. Previous studies have shown that cancerous tumors have enhanced sound speed relative to normal breast tissue (13). This allows for potential differentiation of masses, normal tissue, and fat in these types of images. Attenuation images are tomographic reconstructions based on amplitude changes. Higher attenuation in cancer causes greater absorption or scatter of the US wave, so attenuation in conjunction with sound speed provides a potentially effective means of determining malignancy. Reflection images, based on changes in acoustic impedance, provide echo-texture data and anatomical detail for the entire breast. These three types of images can be combined by means of image fusion, allowing for multi-parameter visual characterization of masses.

2.3 Image Fusion

Image manipulations and calculations were performed with *ImageJ*, a public-domain, java-based image processing program whose development was supported by the National Institutes of Health. A macro in *ImageJ* was developed and used to fuse images and adjust thresholds. Adjusting thresholds regulates the visibility of masses and other breast tissue characteristics relative to general anatomy thereby enabling the suppression of background tissue. This process allowed multiple characteristics to be viewed within a single fused image. Colors could be implemented in order to enhance characterization of lesions and architecture in the fused image. A schematic of the rationale can be seen in Figure 1.

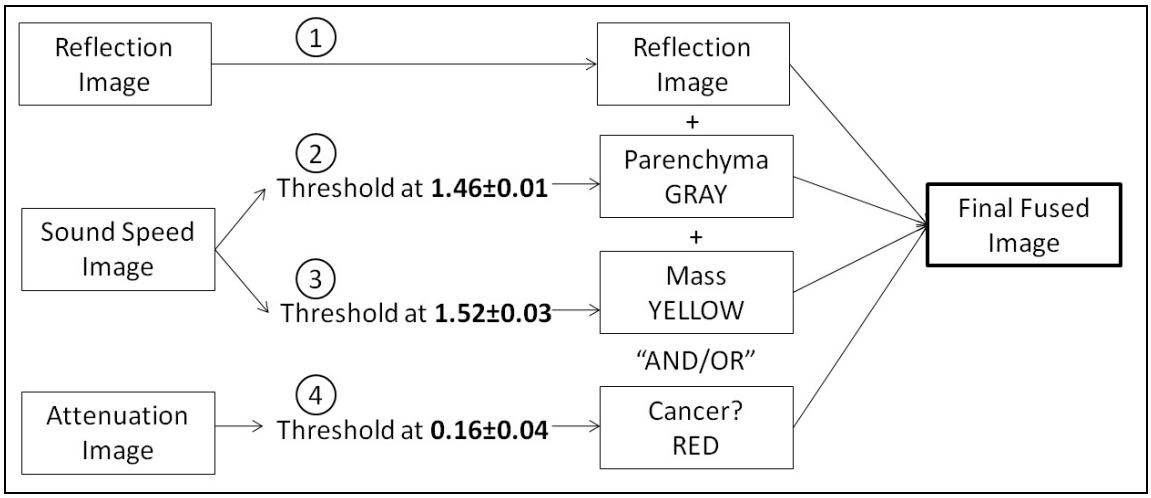

Figure 1: Image Fusion Process

As seen in Figure 1, the first step of the fusion process is to incorporate the reflection image as the background. The sound speed image is then thresholded at two different instances (step 2 and 3 in Figure 1). Applying the threshold of 1.46±0.01 km/s in step 2 will yield architectural features, including fibroglandular tissue and parenchyma, and assign those pixel values to a transparent gray. This image is overlaid on top of the reflection image. The original sound speed image is thresholded again, as seen in step 3, at 1.52±0.03 km/s. This will remove all tissue in the image except for pixels representing a solid mass. Next, as depicted in step 4, the attenuation image is thresholded at 0.16±0.04 dB/cm. The images created at step 3 and 4 are then subjected to either a logical .OR. or .AND. operator in order to generate a final depiction of the solid masses that also differentiates between malignant and benign. Using the logical .OR. operator will determine if there a solid mass exists. This occurs when there is an area of elevated sound speed present, with no attenuation. If there is no elevated attenuation, it can be concluded that this is a benign solid mass (fibroadenoma) and and the fusion algorithm will color it yellow. Finally, using the logical .AND. operator will only display an area that is above both the sound speed and attenuation threshold. Simultaneously exceeding both of those thresholds most likely indicates the presence of cancer, so the algorithm will color this area red and add it to the fused image. Therefore, the final fused image displays overall breast architecture (via reflection), fibroglandular tissue (via sound speed), benign solid masses (via sound speed .OR. attenuation) and suspicious lesions (via sound speed .AND. attenuation), concurrently.

3. RESULTS

A visual assessment of the images led to the identification of parenchyma, fibrous stroma, masses and fatty tissues in both UST and MR images. Components of normal breast anatomy had similar distribution on UST and MR (Figures 2 and 3). The gray-scale in the fused image corresponded directly to the fat-subtracted MR image where dark gray represented fat, light gray parenchyma, and the thin white bands fibrous stroma.

Benign lesions, such as fibroadenomas, not only demonstrated smooth boundaries, but were visible in fused images when a lower attenuation threshold was applied, as well as when the .OR. operation only identified higher sound speed (Figure 2). On the other hand, reflection images provided good detection of the architectural distortion to surrounding filamentous bands and/or connective tissue by cancers (Figure 3).

In Figure 3, both UST and DCE-MR show masses of similar size and extent, located within the same circumferential position. Furthermore, this figure emphasizes UST's ability to accurately image the irregular, invasive margins of a carcinoma extending into parenchymal tissue without the use of contrast enhancement. Comparison of UST with standardized contrast-enhanced fat-subtracted MR images shows that the UST correspond to the masses identified in MR. In all cases when invasive ductal carcinoma (IDC) was present within UST's scanning range our fusion method was able to detect it. DCIS was not part of the dataset for evaluation.

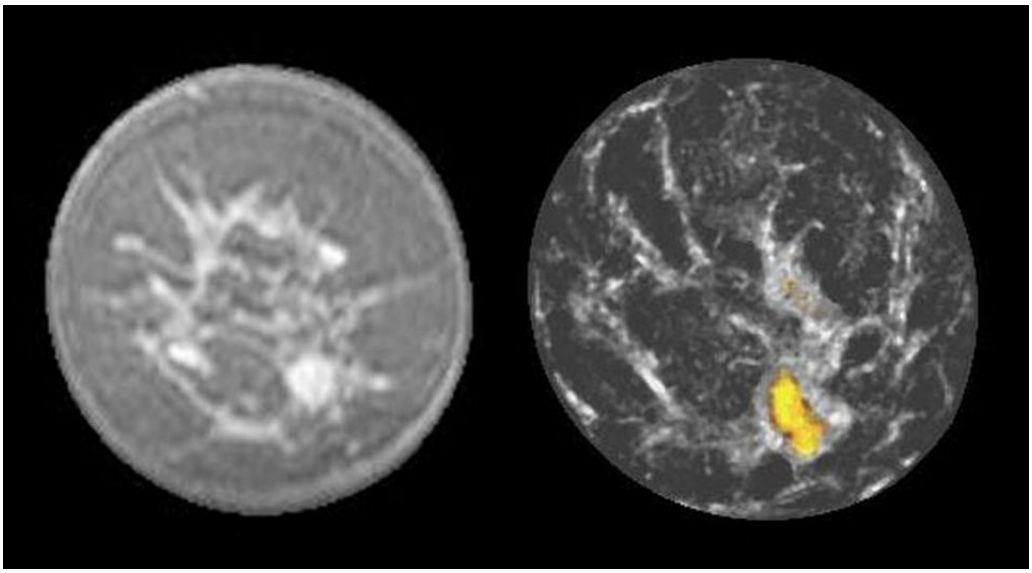

(a) **(b)**

Figure 2: *a.* Coronal fat-subtracted MR image of a female's breast showing a fibroadenoma in the 5:00 position. *b.* Fused UST image of the same patient using the .AND. operator. *b.* Fused UST image of the same patient using the .OR. operator. The fibroadenoma can be seen as yellow in the lower right quadrant.

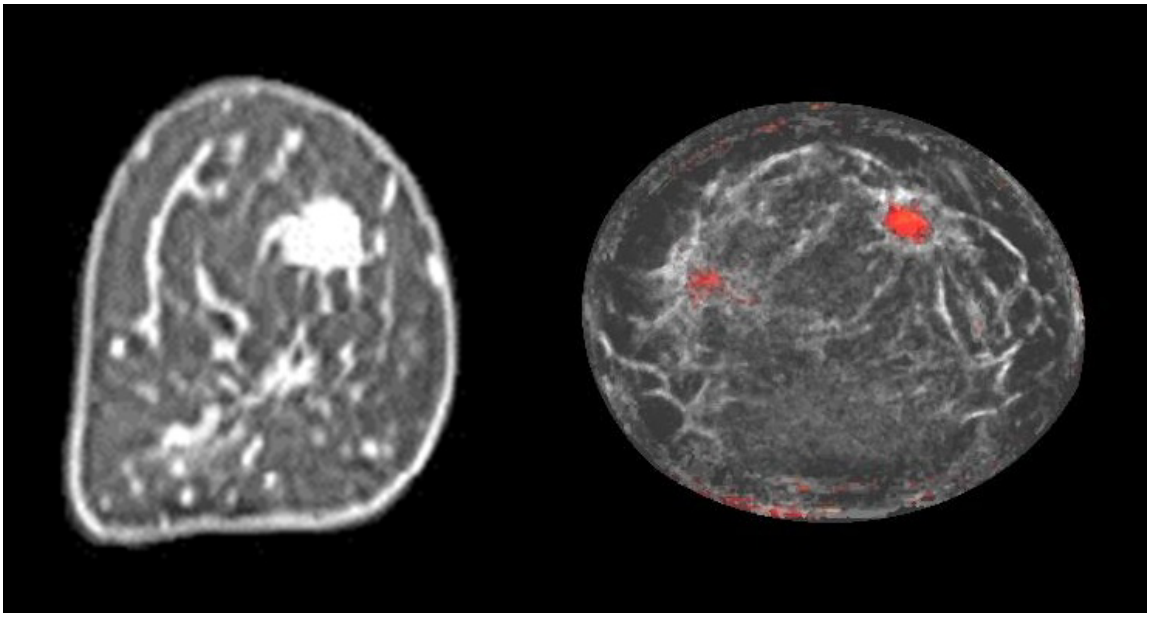

(a) **(b)**

Figure 3: - *a.* Coronal T1 fat-subtracted enhanced MR sequence of a female's breast with a 1.7 cm IDC. *b.* Fused UST image using the .AND. operator. The red area on the UST image shows that the mass in the 1:00 position has high sound speed and attenuation, and closely correlates to the contrast-enhanced image without use of an IV contrast agent. Some parenchyma and/or fibrous band junctions can incidentally reach threshold (9-10:00 position) but are easily excluded as not having mass effect on several slices.

4. DISCUSSION

Tumor extent similar to DCE-MR was shown prospectively by UST when masses simultaneously exceeded thresholds of 1.52±0.03 km/s for sound speed (total variation regularized) and 0.16±0.04 dB/cm in attenuation. Qualitative comparison of the fused UST images with MR sequences using these thresholds showed that UST images had similar mass contrast and overall appearance to that of T_1 fat-subtracted gadolinium-enhanced MR sequences. Anatomical differences can be accounted for by several factors including dissimilar breast deformation under MR (air) and UST (water) examination conditions, a lower spatial resolution of UST images, and greater slice thickness associated with UST images. The concordance of breast anatomy visualized by UST and MR (Figures 2 and 3) suggests that the effect of artifacts and errors associated with UST imaging are modest and do not limit the interpretation of the UST images.

Benign masses tended to have similar properties to normal breast tissue. Consequently, their characterization relied heavily on reflection images to detect smooth margins and fibroadenomas (Figure 2). In addition to their smooth margins on reflection images, fibroadenomas could be visualized in the fused images when using the .OR. operation (Figure 2). Fibroadenomas normally exhibited higher sound speed compared to surrounding tissue but not much attenuation of the acoustic wave due to their lack of homogeneous histology and lack of interaction with surrounding normal tissues. In contrast, cancers showed poor margin discrimination by reflection alone because of the reduced echo contrast of irregular margins due to peripheral invasion and/or tissue interaction. Therefore, the ability of reflection images to display architectural distortion to surrounding filamentous bands and/or connective tissue, as compared to the smooth margins of benign lesions, provides an additional means of predicting malignancy (Figure 3).

Out of a cohort of 36 patients, when a cancerous mass was present and within the scanning range, it was found using the described fusion methodology in all cases. Therefore, differentiation of malignant from parenchymal tissue was achieved without the use of contrast agents. This suggests that ultrasound tomography can effectively detect and characterize various breast lesions in a completely non-invasive manner, even in women with dense breasts. Under such a methodology, a suspicious lesion can be isolated in UST images more consistently than the same lesion in non-contrast MR images. Furthermore, this concordance provides justification for pursuing the UST method with the goal of leveraging its lower intrinsic cost and short exam times.

5. CONCLUSION

This study presents threshold values that may be applied to UST images to depict similar overall breast anatomy to DCE-MR, and provide excellent tumor conspicuity without IV contrast. A strong concordance between UST- and MR-rendered breast anatomy was demonstrated, indicating that UST could provide a lower-cost alternative to MR for both diagnosis and volume-based assessments of breast characteristics. Further study with a larger cohort of patients will be performed to fine-tune our values and automate the image fusion process as the prototype is prepared for multi-center clinical trials and a commercialized product.

ACKNOWLEDGMENTS

The authors acknowledge that this work was support by a grant from the Michigan Economic Development Corporation (Grant Number 06-1-P1-0653). For correspondence regarding this paper, contact Neb Duric at *duric@karmanos.org*.

6. REFERENCES

[1] Lehman CD, Isaacs C, Schnall MD, Pisano ED, Ascher SM, Weatherall PT, et al. Cancer yield of mammography, MR, and US in high-risk women: prospective multi-institution breast cancer screening study. Radiology 2007; 244:381-388.

[2] Schnall MD. Breast imaging technology: Application of magnetic resonance imaging to early detection of breast cancer. Breast Cancer Res 2001;3:17-21.

[3] Kuhl CK, Schild HH. Dynamic image interpretation of MRI of the breast. J Magn Reson Imaging 2000;12:965-74.

[4] Moore SG, Shenoy PJ, Fanucchi L, et al. Cost-effectiveness of MR compared to mammography for breast cancer screening in a high risk population. BMC Health Serv Res. 2009;9:9.

[5] Duric N, Littrup P, Poulo L, et al. Detection of breast cancer with ultrasound tomography: First results with the computerized ultrasound risk evaluation (CURE) prototype. Med. Phys. 2007;34(2):773-85.

[6] Duric N, Littrup P, Babkin A, et al. Development of ultrasound tomography for breast imaging: technical assessment. Med. Phys. 2005;32(5):1375-86.

[7] Li C, Duric N, Littrup P, Huang L. In vivo breast sound-speed imaging with ultrasound tomography. Ultrasound in Med. & Biol. 2009;35(10):1615-1628.

[8] Glide-Hurst CK, Duric N, Littrup P. Volumetric Breast Density Evaluation from Ultrasound Tomography Images. Med Phys. 2008;35(9):3988-97.

[9] Glide-Hurst CK, Duric N, Littrup P. A New Method for Quantitative Analysis of Mammographic Density. Med Phys. 2007;34(11):4491-8.

[10] Goss SA, Johnston RL and Dunn F. Comprehensive compilation of empirical ultrasonic properties of mammalian tissues. J Acoust Soc AM 1978; 64: 423-457.

[11] Ranger B, Littrup P, Duric N, et al. Breast Imaging with acoustic tomography: a comparative study with MRI. Proceedings of the SPIE. Medical Imaging 2009: Ultrasonic Imaging and Signal Processing Vol. 7265**.**

[12] ImageJ Web site. http://rsbweb.nih.gov/ij/. Accessed August 2, 2009.

[13] Schreiman JS, Gisvold JJ, Greenleaf JF, Bahn RC. Ultrasound transmission computed tomography of the breast. Radiology 1984; 150:523-30.